buildings

MDPI

Article

Microstructure and Mechanical Properties of Cost-Efficient 3D Printed Concrete Reinforced with Polypropylene Fibers

Dragoș Ungureanu [1,2,*], Cătălin Onuțu [1], Nicolae Țăranu [1,2], Nicoleta Vornicu [3], Ștefan Vladimir Zghibarcea [1], Dan Alexandru Ghiga [1] and Ionuț Alexandru Spiridon [1]

[1] Faculty of Civil Engineering and Building Services, "Gheorghe Asachi" Technical University of Iaşi, 43 Mangeron Blvd., 700050 Iaşi, Romania; catalin.onutu@academic.tuiasi.ro (C.O.); nicolae.taranu@academic.tuiasi.ro (N.Ț.); stefan.zghibarcea@holcim.com (Ș.V.Z.); danghiga@hotmail.com (D.A.G.); ionut-alexandru.spiridon@student.tuiasi.ro (I.A.S.)
[2] The Academy of Romanian Scientists, 3 Ilfov Street, 030167 Bucharest, Romania
[3] Metropolitan Center of Research T.A.B.O.R., 9 Closca Str., 700066 Iaşi, Romania; cmctaboriasi@yahoo.com
* Correspondence: dragos.ungureanu@staff.tuiasi.ro

Abstract: Studying emerging and cutting-edge digital construction techniques, especially the utilization of 3D printing for concrete/mortar materials, holds significant importance due to the potential benefits that these technologies might offer over the traditional approach of casting concrete in place. In this study, a mixture composed of Portland cement, water, sand, limestone filler and polypropylene fibers was utilized for 3D printed concrete production towards the sustainable constructions approach. The benefits that sustain this statement include reduced construction time and material requirements, diminished error and cost, increase in construction safety, flexibility of architectural design, and improved quality with much less construction cost and waste. The microstructure, fresh and hardened mechanical properties of the polypropylene fiber reinforced 3D concrete were investigated. The results indicated that it is essential to attain a slump measurement of approximately 40 mm and a slump flow within the range of 140 to 160 mm, as stipulated by relevant standards (ASTM C1437 and C230/C230 M), in order to create a 3D concrete mixture suitable for extrusion. Also, the effects of printing parameters, fiber dosage, material composition, and other factors on the 3D printed concrete strength were discussed, and the corresponding adjustments were addressed.

Keywords: 3D concrete printing; microstructure; printability; mechanical properties; buildability performance

check for updates

Citation: Ungureanu, D.; Onuțu, C.; Țăranu, N.; Vornicu, N.; Zghibarcea, Ș.V.; Ghiga, D.A.; Spiridon, I.A. Microstructure and Mechanical Properties of Cost-Efficient 3D Printed Concrete Reinforced with Polypropylene Fibers. *Buildings* **2023**, *13*, 2813. https://doi.org/10.3390/buildings13112813

Academic Editor: Yanping Zhu

Received: 8 September 2023
Revised: 25 October 2023
Accepted: 8 November 2023
Published: 9 November 2023

Copyright: © 2023 by the authors. Licensee MDPI, Basel, Switzerland. This article is an open access article distributed under the terms and conditions of the Creative Commons Attribution (CC BY) license (https://creativecommons.org/licenses/by/4.0/).

1. Introduction

Projections suggest that the world's population will reach approximately 9.7 billion by 2050 [1], leading to a significant need for infrastructure and budget housing. This scenario imposes a tight timeframe for meeting these developmental demands. At this point, to meet the housing demand, an annual requirement of almost 30 million houses is necessary. As a consequence, the construction sector faces immense pressure in dealing with both the extensive need for infrastructure and the environmental degradation associated with concrete traditional cast in-place methods. Furthermore, there are significant concerns that require significant attention. These include high rates of accidents and injuries, heavy reliance on labor, low efficiency, endless increasing of the construction costs, and the substantial cost of formwork, which, in some cases, accounts for nearly 30% to 50% of the total construction cost [2]. In addressing these concerns, researchers are directing their efforts toward adopting innovative and cutting-edge digital technologies. These technologies aim to accelerate the construction process, reduce construction costs, and promote safety while minimizing or eliminating the need for formwork. Within this context, 3D printing, a form of additive manufacturing, emerges as one of the most promising construction techniques in recent years [3].

The utilization of 3D printing in civil construction involves a range of methods for producing structural elements, with a primary focus on 3D concrete printing (3DCP) [1–3]. These methods include material extrusion, binder jetting, material jetting, and powder bed fusion. Among these techniques, 3DCP utilizing extrusion is currently the most extensively researched.

Presently, numerous research teams worldwide are actively engaged in this topic, and several have made notable progress. The majority of these investigations have primarily concentrated on assessing the properties of fresh materials or properties during the early stages (typically within hours) of development [4–6]. The primary objective has been to successfully manufacture elements or structures. As a next step, it was mandatory to ensure that the 3DCP has convenient mechanical properties. Thus, numerous studies have been undertaken, aiming to incorporate reinforcement into 3DCP elements. These efforts include the use of additive concrete, which involves materials like limestone filler, calcium sulfoaluminate cement, and cellulose fiber to enhance the overall strength and the interlayer properties of the 3DCP elements [7,8]. Additionally, heightening the mechanical performance of concrete has been explored by embedding fiber reinforced polymer bars, laminates, or micro-cables during the printing process [9–11]. Furthermore, the optimization of 3DCP workability has been pursued by incorporating solid waste materials such as gypsum, biochar, carbide slag, red mud, aluminum ash, and ashes from municipal solid waste incineration into the mixtures [12,13].

Although they have provided solutions to the performance requirements of 3D printed concrete, the methods mentioned above have significantly contributed to the increase in the cost per cubic meter of printed concrete. The incorporation of carbon, aramid, or basalt fibers, combined with the addition of silica fume, are just a few of the aspects that have led to rising costs. In this context, the savings achieved in construction time, formwork, and labor become irrelevant. On the other hand, using polypropylene fibers as an alternative to incorporating carbon, aramid, or basalt fibers in 3D printed mortars presents a highly viable and advantageous choice. Polypropylene fibers offer a range of benefits, making them an attractive option for reinforcing mortars. First, polypropylene fibers are readily available and cost-effective, making them an economical choice for construction projects. They also provide excellent resistance to chemical corrosion and are highly durable, ensuring the longevity of the 3D printed structure. Additionally, polypropylene fibers have a low density and are lightweight, which can improve the workability of the mortar mix and reduce the overall weight of the printed components, without compromising structural integrity. Moreover, they enhance crack resistance and reduce shrinkage, leading to a more robust and reliable end product. Their ease of handling and compatibility with the 3D printing process make polypropylene fibers a practical and sustainable solution for reinforcing 3D printed mortars, without the expense and complexity associated with other fiber types.

This study underscores the considerable potential of 3D printed concrete as a cost-effective alternative for construction projects. It also presents a comprehensive analysis of 3D printed concrete, encompassing the formulation and preparation method, morphological and microstructural examinations, evaluations of the properties of freshly mixed 3D concrete, and assessments of the properties of hardened 3D concrete. Furthermore, it underscores the critical importance of optimizing concrete mixtures, demonstrating that achieving cost-efficiency is not exclusively dependent on prefabrication but is significantly influenced by the selection of materials. These findings pave the way for new possibilities in sustainable, economical, and high-performance construction practices in the years to come.

2. Materials and Mix Proportioning

The materials selected for the study were natural quartz sand with a particle size of 0–1 mm, CEM II/A-S 52.5 R Portland slag cement, and limestone filler extracted from a nearby quarry basin (Figure 1). The mixture incorporated two types of additives: a viscosity-modifying agent in the form of an aqueous solution combined with a high-molecular-weight synthetic copolymer, and a super-plasticizer designed to accelerate strength development

during the initial stages of hydration, even when exposed to low environmental temperatures and heat curing. The super-plasticizer is a high-range water-reducing admixture that enables a significant reduction in water content without sacrificing the workability of the 3D concrete mix. This means that the cement particles are more efficiently dispersed in the mix. Better dispersion enhances the contact between water and cement particles, which promotes more rapid and uniform hydration. Additionally, the use of the super-plasticizer reduces the size and number of capillary pores in the 3D concrete printed elements. Smaller capillaries limit the ingress of water and the movement of aggressive substances, helping to densify the 3D concrete matrix and enhance early strength development. The water-to-cement ratio was consistently maintained at 0.457, a ratio previously determined to yield the optimal compressive strength progression [3]. These additives were incorporated into the 3DCP mix to tailor and optimize the workability/rheological properties (i.e., extrudability, pumpability, and thixotropy) to meet the 3DCP performance requirements. Monofilament polypropylene fibers of considerable length (12 mm), whose characteristics are detailed in Table 1, were introduced into the 3DCP mixture [14]. This addition served the purposes of mitigating plastic shrinkage cracking, enhancing resilience, and bolstering post-cracking performance in both tensile and flexural situations [15,16].



Figure 1. Raw materials.

Table 1. Properties of the monofilament polypropylene fibers.

Filament Type	Length [mm]	Equivalent Diameter [μm]	Tensile Strength (According to the Manufacturer) [N/mm^2]
mono	12	21–34	≥300

The concrete mix was prepared using a handheld electrical mortar mixer with adjustable speed in a controlled laboratory setting. The procedure aimed to achieve a homogenous and robust concrete mix while avoiding material trapping at corners, as crucial steps in ensuring the mix's quality and performance (Table 2). The mix design is shown in Table 3.

Table 2. Mixing method.

Mixing Sand, Limestone Filler, and Polypropylene Fibers (5 min)
• The first step involved placing sand, limestone filler, and polypropylene fibers into a cylindrical tank. • A handheld electrical mortar mixer, equipped with an adjustable speed setting, was employed. • Initially, the mixer was set to a low speed, and the mixture was blended for 5 min to ensure an even distribution of the components.
Gradually Increasing Mixer Speed (Up to 350 RPM)
• Mixer speed was progressively increased to 350 RPM to uniformly integrate all components. • The choice of a cylindrical tank was critical to prevent material entrapment in corners, thereby enhancing the mix's consistency.

Table 2. *Cont.*

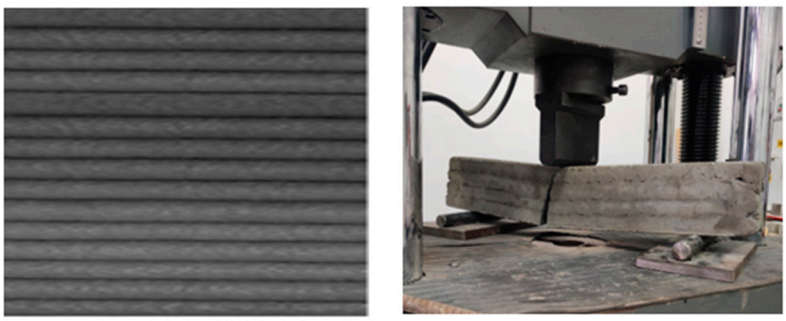
Adding Half of the Water (5 min at 500 RPM)
• Half of the required water was added to the mixture. • Mixer speed was elevated to 500 RPM for an additional 5 min, enhancing workability and consistency.
Incorporating Cement and the Remaining Water (5 min at 700 RPM)
• Cement was introduced into the mix, followed by the addition of the remaining water. • Mixer speed was raised to 700 RPM for 5 min.
Introducing Viscosity-Modifying Agent and Plasticizer (7 min at 700 RPM)
• The next stage involved introducing the viscosity-modifying agent and plasticizer. • Mixer speed was maintained at 700 RPM for 7 min to optimize concrete viscosity and workability.

Table 3. Mix design.

Cement [kg]	Water [L]	Sand [kg]	Limestone Filler [kg]	Fibers [kg]	Viscosity Modifying Agent [%]	Superplasticizer [%]
580	265	1358	200	1	0.4	1.1

3. Printing Stage

The chosen printing method is extrusion-based and employs a 3D piston system printer with three translational degrees of freedom [17]. This printer offers a full 360-degree printing capability through continuous rotation and is fitted with circular nozzles of varying diameters (3 mm, 5 mm, and 20 mm). Following nozzle attachment, the extruder was filled with the concrete mixture and primed meticulously to ensure the extrusion process occurred without any trapped air (voids) or tearing at the nozzle. A consistent printing speed of 60 mm/s was selected, and the layer thickness was adjusted between 3 mm and 20 mm based on the specifications of the printed project. With these settings, the printer successfully produced various items, including wall panels (to evaluate the mix's buildability), (Figure 2a), architectural elements (to assess its capacity for intricate model manufacturing), and specimens (to test the mix's mechanical strength), (Figure 2b). The layer height for the wall panel illustrated in Figure 2 is 15 mm. Each layer was 500 mm long. In total, over 100 layers were printed without showing any sign of premature collapse.



(a) (b)

Figure 2. 3D printing: (**a**) wall panel, (**b**) specimen for the three-point bending test.

4. Morphology and Microstructure

Analyzing the morphology and microstructure of 3D printed concrete is essential for optimizing its quality, performance, and durability. X-ray Fluorescence (XRF) spectroscopy is a powerful tool for characterizing the elemental composition of 3D printed concrete,

aiding in the assessment of its microstructural properties. By combining morphological and microstructural insights with XRF analysis, researchers and engineers can enhance the design, production, and performance of 3D printed concrete structures, further advancing the potential of this innovative construction technology.

The specimens subjected to the microscope analyses were prepared by cutting 10 × 10 mm sections from larger prism specimens measuring 100 mm × 100 mm × 500 mm. These larger specimens were originally printed and subjected to the three-point bending tests at 28 days of age. The layer height used for printing these specimens was 15 mm, and a 20 mm nozzle was used.

Through microscopic analysis of the 3D printed concrete samples, several key features have been elucidated. These include the shapes and dimensions of the aggregates, the presence of microcrystalline carbonate binder, as well as the existence of small spherical pores and xenomorphic pores (Figure 3a). Additionally, in detailed microscope images, an exceptionally strong cohesion between the aggregate and the calcitized binder has been observed, with minor remnants of Portland cement clinker (Figure 3b). The pores appear to be spherical and isolated.

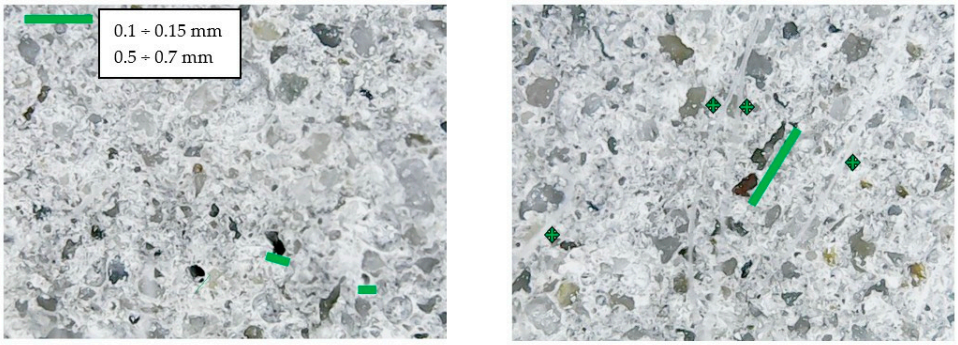
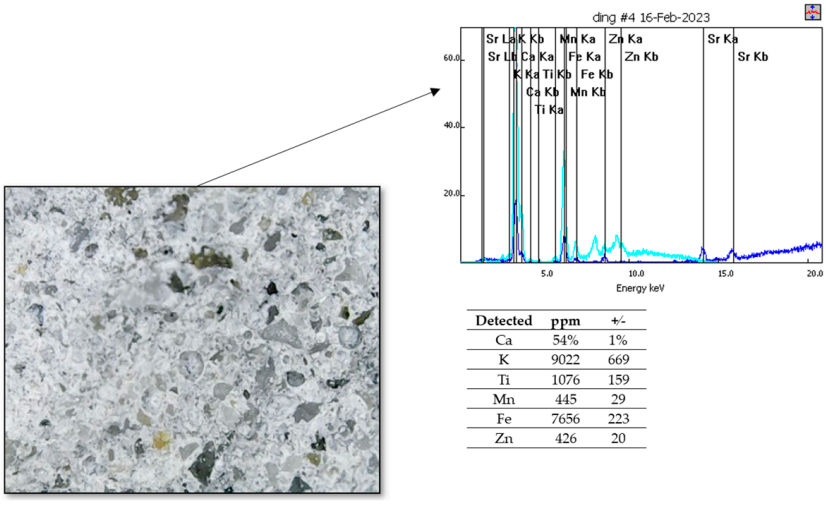


Figure 3. Microscopic analysis of 3D printed specimens (500 X): (**a**) shapes and dimensions of the aggregates, (**b**) strong cohesion between the aggregate and the calcitized binder.

The morphology of the materials was examined using an isotope-free XRF spectrometer from GP Technical Equipment, Georgia, USA, specifically the Innov X model, in conjunction with a mini-PC. This setup was utilized to ascertain the chemical properties and validate the chemical composition of particles, as depicted in Figure 4.



Detected	ppm	+/-
Ca	54%	1%
K	9022	669
Ti	1076	159
Mn	445	29
Fe	7656	223
Zn	426	20

Figure 4. X-ray spectrum and elemental composition of the 3D printed concrete.

Under microscopic examination, it is obvious that the adhesion between the aggregate and the binder is exceptionally strong, and that the polypropylene fibers are arranged in a parallel pattern (Figure 5). This adhesion boundary is often prominently marked by microcrystalline calcite, indicating excellent cohesion between the components. The morphology and microstructure analysis revealed the following findings:

Natural Aggregate:

- The natural aggregate is polymictic, consisting of both grainclast and lithograins;
- Morphologically, it exhibits angular, subangular, and rounded shapes, with grain sizes ranging from approximately 0.1 to 1 mm;
- Grainclasts are predominant and comprise the following minerals: quartz (in abundance), feldspars, frequently perthitic microcline, biotite, and muscovite;
- Lithoclasts are rare.

Binder:

- The analysis identified a microcrystalline calcite binder, resulting from carbonation;
- The $CaCO_3$ (calcite) and $CaFe(CO_3)_2$ carbonates were identified in the binder;
- Hydroxylated cryptocrystalline calcium silicates and minor un-hydrated remnants of Portland cement clinker are present.

Pores:

- The pores exhibit both spheroidal and xenomorphic characteristics;
- Spherical pores come in varying sizes: very small pores (0.1 ÷ 0.18 mm) are the most common and can be found paired together, while larger pores (0.3 ÷ 0.5 mm) are isolated;
- Xenomorphic pores vary in size and are infrequent;
- All pores are finely lined with microcrystalline calcite.

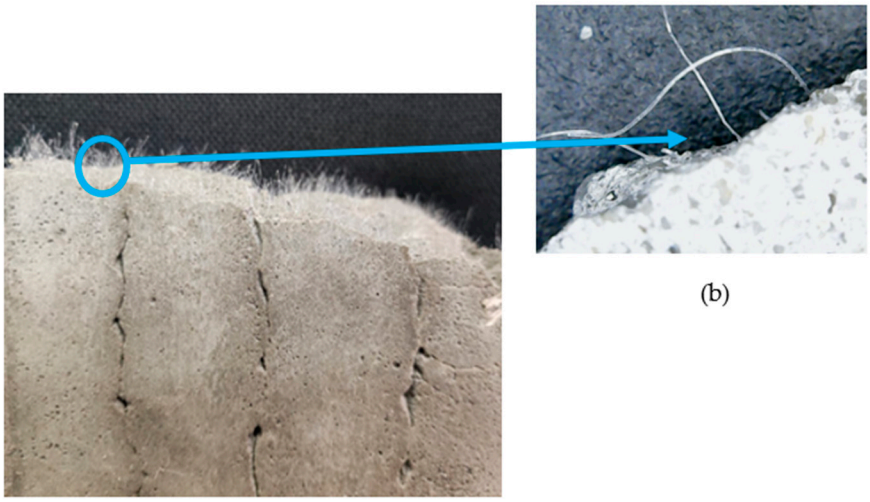


Figure 5. Reinforcements: (**a**) Orientation of the polypropylene fibers, (**b**) 500 X—View.

5. Properties of Freshly Mixed 3D Concrete

In a general context, non-extrudable mixtures display a notably higher frequency of surface defects on the extruded filament compared to mixtures that can be extruded. However, in the context of this research, we evaluated the extrudability of the specific 3D concrete under study by quantifying the visible surface defects present on the top surface of the extruded filaments during the printing process. These evaluated defects are only the ones that are discernible to the naked eye (Figure 6).

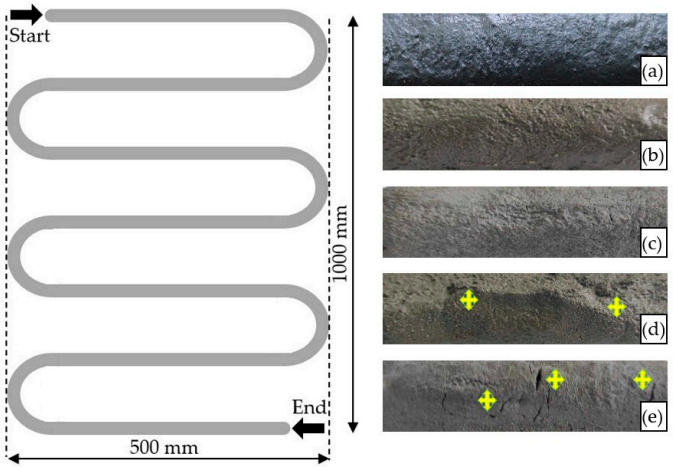


Figure 6. Printing path to determine extrudability: (**a**) appearance and texture during printing, (**b**) appearance and texture 10 min after printing, (**c**) appearance and texture of hardened 3D concrete, (**d**,**e**) appearance and texture of some mixes tested in the design process, which exposed visible defects.

As can be observed in Figure 6a–c, the concrete printing along the established path was carried out without detecting any visible defects in the filament. In the case of other mixes, tested by the authors prior to the development of the final recipe, visible defects were indeed detected. These defects are depicted in Figure 6d,e for comparative purposes in order to underscore the extrudability of the material presented in this study. The parameters imposed during the testing are outlined in Table 4.

Table 4. Printing parameters.

Printing Speed [mm/s]	Layer Height [mm]	Nozzle [mm]
60	15	20

It is worth noting that a previous study conducted by the authors [3] demonstrated that this particular mix can also be utilized with a 3D printer lacking an extruder. However, under such circumstances, the technology is primarily suitable for manufacturing projects with simple geometries involving linear paths, and it may face limitations when attempting to create complex architectural models.

Flowability, in the context of 3DCP, is defined as the material's capacity to effortlessly flow and occupy a given space under its self-weight. Within 3DCP, the concept of flowability holds significance as it plays a pivotal role in ensuring a consistent manufacturing process, contributing to the reduction of printing anomalies and the prevention of blockages. In this study, the flow characteristics of the mix were assessed by slump measurements, as per the guidelines specified in the European Standard EN 12350-2:2019 [18]. The slump measurement (40 mm) was determined by calculating the average difference in height between the initial height of the cone and the height of the 3D concrete after deformation. The obtained value (40 mm) is also indicated by previous research, which concluded that 3D concrete mixtures should ideally exhibit slump values falling within the range of 40 to 60 mm [19].

The slump test exhibits certain constraints, particularly when applied to the context of 3DCP. This test does not adequately address the material's shear-thinning behavior, leading to potentially inaccurate measurements. Consequently, slump flow tests were conducted, as they are better suited for assessing the flowability of 3D concrete materials, taking into consideration their shear-thinning behavior. These tests were performed following the guidelines specified in the ASTM C1437 and C230/C230 M standards [20,21], and the

resulting measurement (160 mm) holds significance within 3DCP applications, as indicated by previous research [19].

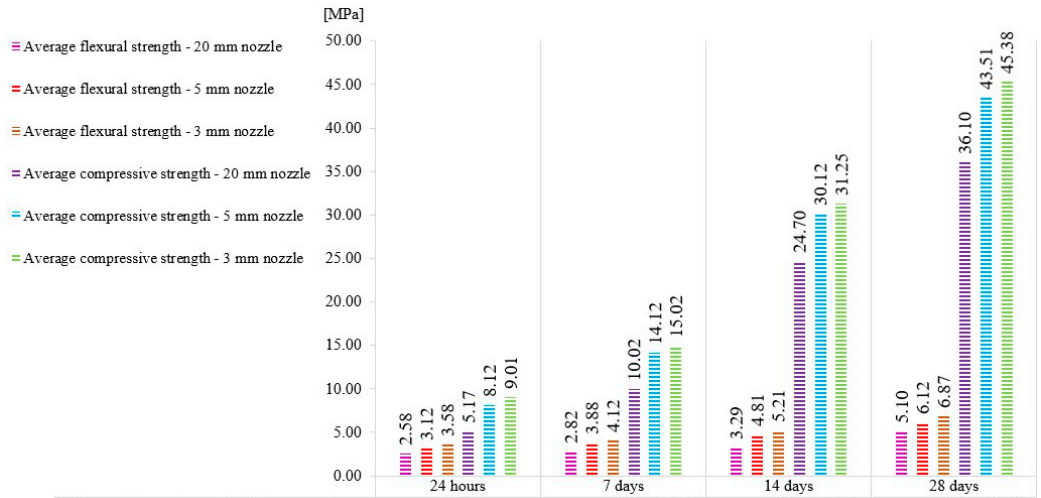
Buildability stands as the primary criterion when assessing a printable concrete mixture. In fact, a printed concrete material possessing adequate buildability must maintain its form without undue distortions and exhibit tolerable settling in its lower layers. The buildability assessment is a widely used method for evaluating 3D-printed materials, enabling researchers to ascertain the maximum number of layers that can be stacked without causing the structure to collapse. Using the mix detailed in this study, more than 100 layers were printed without any discernible indications of instability or structural breakdown (Figure 2a), employing the identical printing parameters as those outlined in Table 4. The layer height for the wall panel was 15 mm. Each layer was 500 mm long.

6. Properties of Hardened 3D Concrete

The assessment of the development of compressive strength (f_c) in printed concrete cubic samples (100 mm on each side), with an average density spanning from 2131.5 kg/m^3 to 2249.8 kg/m^3, was conducted following 24 h, as well as 7, 14, and 28 days of curing, in accordance with the SR EN 12390-3:2002 standard [22]. The tests were performed at a loading rate of 0.5 mm/min and preceded by a pre-load of 20 N before commencement. It is worth noting that the study referenced in [15] has validated these parameters specifically for the compressive strength testing of 3D concrete/mortar materials. This research [15] demonstrated that when these parameters are applied, the tests consistently yield reliable and replicable results.

Three-point bending tests were performed on prism specimens (100 mm × 100 mm × 500 mm) at four different time intervals, 24 h, 7 days, 14 days, and 28 days, adhering to the guidelines outlined in SR EN 12390-5:2019 standard [23]. The tests were conducted using a crosshead loading rate of 0.25 mm/min, with data acquisition occurring at a constant rate of 10 Hz.

Figure 7 depicts the variations in compressive and flexural strengths at specific time intervals (24 h, as well as 7, 14, and 28 days), with these variations being influenced by the nozzle used. A total of 120 specimens were tested (5 for each nozzle size, for each test, at specific time interval).



	24 hours	7 days	14 days	28 days
Average flexural strength - 20 mm nozzle	2.58 [MPa]	2.82 [MPa]	3.29 [MPa]	5.10 [MPa]
Average flexural strength - 5 mm nozzle	3.12 [MPa]	3.88 [MPa]	4.81 [MPa]	6.12 [MPa]
Average flexural strength - 3 mm nozzle	3.58 [MPa]	4.12 [MPa]	5.21 [MPa]	6.87 [MPa]
Average compressive strength - 20 mm nozzle	5.17 [MPa]	10.02 [MPa]	24.70 [MPa]	36.10 [MPa]
Average compressive strength - 5 mm nozzle	8.12 [MPa]	14.12 [MPa]	30.12 [MPa]	43.51 [MPa]
Average compressive strength - 3 mm nozzle	9.01 [MPa]	15.02 [MPa]	31.25 [MPa]	45.38 [MPa]

Figure 7. Properties of hardened 3D concrete.

7. Cost Calculation Approach for 3D Concrete Printing in Conjunction with the Internet of Things

The technology of 3DCP serves as the foundational framework for implementing the Internet of Things (IoT) in the construction sector [24,25]. The widespread adoption of IoT in construction, facilitated by 3D printing, becomes more feasible when either the cost of 3DCP is low or the efficiency of its output significantly outweighs the input [26]. To achieve this, it is imperative to gain a comprehensive understanding of the costs associated with 3DCP and strategies to minimize them. This understanding is crucial for formulating precise development strategies for IoT in the construction industry, ensuring accessibility to a broader spectrum of companies, rather than restricting its usage to larger entities. Thus, a thorough examination of the cost calculation methodology and structure in construction is indispensable. While conventional construction has well-established global standards for cost calculation, 3DCP lacks a structured bill of quantities, budget estimates, and pricing foundations, leading to complexities in cost assessment. Furthermore, research endeavors aimed at enhancing the strength properties of 3D printed concrete elements tend to narrow the range of applications for this technology. The utilization of high-performance materials like carbon and basalt fibers or silica fume incurs substantial costs. This cost disparity necessitates a comparative analysis between conventional construction methods and 3D printing, as outlined in Table 5 [27].

Table 5. Cost categories. Comparison between convention constructions and 3D printing.

Cost Categories	Traditional/Conventional Constructions	Offsite Printing (Precast Members)		Onsite Printing
		Printing	Assembling	
Labor	X		X	X
Machine	X		X	
Material	X		X	X
Health and safety measurements	X		X	X
Night shifts	X			X
Additional cost for the winter season	X			X
Equipment	X		X	X
Equipment protection/maintenance	X		X	X
Scaffolding	X			
Formwork	X			
Discharge (pollution fee)	X			X
Management	X	X		X
Tax	X	X		X
Profit	X	X		X

All costs of producing 3D printed precast elements are included in the "Assembling" category for off-site printing. In the case of offsite printing, many of the costs traditionally associated with on-site construction are minimized or even eliminated. Labor costs encompass salaries, allowances, and insurance. Taxation is determined differently, in accordance with each country's regulatory authorities. Calculating transportation costs for printed components offers two practical methods. One approach entails the printing company assuming responsibility for delivery, with the delivery cost considered part of manufacturing expenses, subject to a value-added tax (VAT). The alternative involves subcontracting transportation to a logistics company, also subjected to VAT. The applicable VAT rates are determined based on specific circumstances.

Onsite 3D printing of buildings remains uncommon due to its relatively recent emergence as a technology. The absence of standards or technical frameworks in 3D construction printing complicates matters. High initial investments and limited market demand make it challenging for construction companies to undertake mass production using 3D printing. In essence, only large corporations can afford to invest in onsite 3D printers, often developing their own concrete mixes to keep final product costs as low as possible and their profit as high as possible (even higher than the one associated with conventional constructions). Consequently, it becomes evident that, contrary to what some scientific articles may suggest, this technology is not a sustainable alternative for social housing but rather a marketing term.

Conversely, offsite printing offers a considerably more cost-effective solution, with equipment typically priced between 10,000 and 70,000 EUR. Additionally, because the printing process occurs within a controlled environment, quality management is significantly more precise, and there are no concerns about environmental factors adversely affecting the machinery. The offsite printing method minimizes material waste as the concrete members are printed with high precision, using only the necessary materials. Onsite 3D printing, due to its real-time nature, may lead to material wastage and increased costs. Furthermore, precast 3D printed concrete members can be tailored to project specifications with ease. Design changes and customizations are more readily accommodated, offering greater flexibility compared to onsite 3D printing, which can be more restrictive in this regard. Offsite printing consists of two distinct phases: component printing and on-site assembly, both associated with industrial construction products. The labor and material expenses incurred during component manufacturing cannot be included in the labor and material costs of the assembly stage. This is because printed components fall within the manufacturing industry, and their labor and material costs are already incorporated into the components themselves.

In addition to the aforementioned factors, in the case of the 3D concrete analyzed in this study, cost optimization does not solely rely on the prefabrication of printed elements but also on the concrete recipe itself. For this reason, the concrete mix was meticulously designed to exclude costly additives or constituents, such as silica fume, basalt and carbon fibers, and carbon nanotubes. Nevertheless, the physical and mechanical performances of this 3D concrete remain comparable, if not superior, to other printable mixtures that incorporate expensive materials.

More expensive mixes may lead to lighter structures, which can have cost implications in the context of a whole project. However, it is essential to recognize that the mix developed in this work is specifically intended for the construction of single-story dwellings. In this case, the typical structural optimization strategies aimed at achieving lighter multi-story structures, and the associated cost reductions, may not be directly applicable or valid. Single-story dwellings have distinct structural requirements, often emphasizing stability, load-bearing capacity, and resistance to environmental factors such as seismic forces and extreme weather. The mix composition for such structures must cater to these specific demands. While more expensive mixes might indeed lead to lighter structures in different architectural contexts, the priorities of single-story dwellings may necessitate a different approach.

Figure 8 provides a comparative analysis of the cost per cubic meter of the 3D concrete investigated in this research in contrast to prices resulting from the addition or substitution of various materials. The presented prices represent the average values of these materials and were obtained through an analysis of the major retail suppliers from Romania.

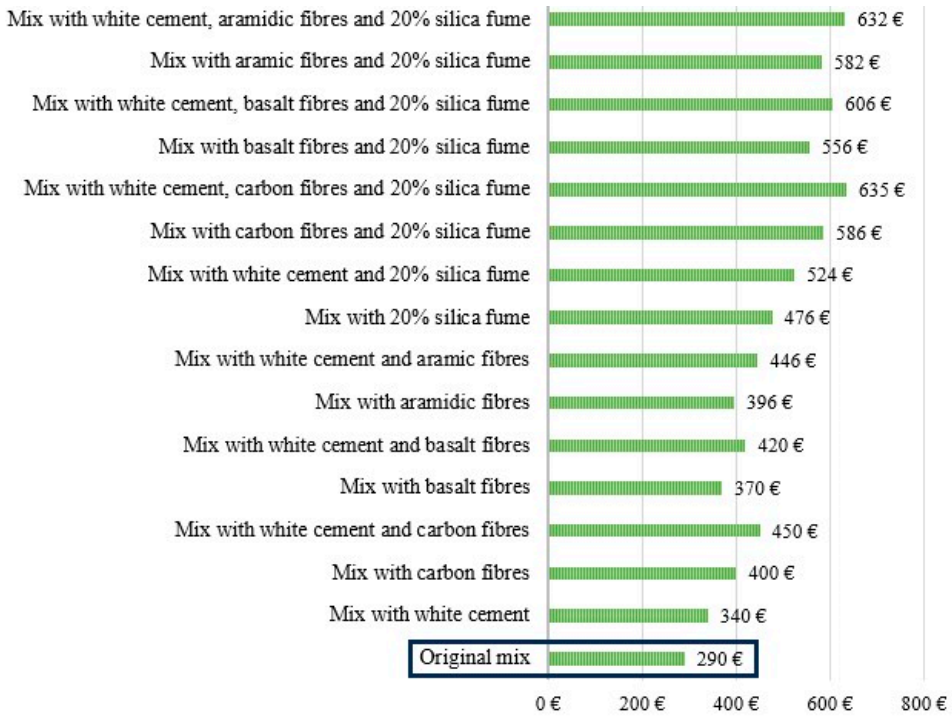


Figure 8. Comparative analysis of the cost per cubic meter of the 3D concrete.

8. Future Research Directions

Despite the significant success achieved in the development of 3DCP technology, this study has identified several challenges that merit further consideration and exploration in future research.

One of the primary future research directions is to extend the applicability of 3DCP technology by designing innovative methods for retrofitting masonry structures using 3D printed materials. While 3DCP has shown promise in building construction, it has the potential to revolutionize the restoration and reinforcement of historical and aging masonry structures. Our goal is to develop techniques and materials that enhance the structural integrity and durability of these heritage buildings while preserving their architectural significance [28–30].

The construction industry is continually evolving, and the demand for efficient and sustainable road infrastructure is on the rise. To meet these demands, we aim to design and produce 3D printed prefabricated elements that are compatible with road construction projects. These elements will incorporate the latest advancements in material recycling technologies, contributing to environmentally friendly and cost-effective road construction practices [31–34].

Concrete, even in its 3D printed form, remains a fundamental construction material. To further improve its structural performance and versatility, we intend to develop novel reinforcement systems akin to the composite systems used in strengthening applications of reinforced concrete structures [35–37]. These systems will optimize the mechanical properties of 3D printed concrete, ensuring it can withstand a wide range of loads and environmental conditions.

Sustainability is a central concern in modern construction practices. Therefore, we plan to explore ways to integrate recycled materials into the recipe for 3D printed concrete. By doing so, we aim to reduce the environmental footprint of construction and promote circular economy principles [38–40].

To advance the understanding of 3D printed concrete and its behavior under various conditions, we intend to develop dedicated numerical models [41,42]. These models will facilitate in-depth analysis and simulations, enabling us to predict and optimize the

performance of 3D printed structures. These simulations will also guide the development of new construction techniques and materials.

9. Conclusions

This study has demonstrated the feasibility and potential of 3D printed concrete made from affordable materials, showcasing comparable or even superior mechanical properties when compared to their expensive counterparts. Based on the experimental program described in this work, the following conclusions can be drawn:

- In printed 3D concrete, which can have complex geometries, polypropylene fibers help control and mitigate cracks that may develop due to various factors, such as the layering process.
- In 3D concrete printing, where precise layering is critical, polypropylene fibers help reduce plastic shrinkage cracking during the printing process. This contributes to the quality and appearance of the 3D-printed concrete surface.
- Polypropylene fibers improved the workability of the 3D concrete mix, making it easier to extrude and shape during the printing process while maintaining its structural properties.
- The mechanical strengths continued to improve over time, with positive trends observed at 24 h, 7 days, 14 days, and 28 days for all nozzle sizes studied.
- The use of 3D printing nozzles of different diameters resulted in notable improvements in mechanical strength. The tensile strength at 28 days increased by 19.61% for the 5 mm nozzle and by 34.12% for the 3 mm nozzle compared to the 20 mm nozzle. Similarly, the compressive strength at 28 days exhibited a 20.66% increase for the 5 mm nozzle and a 25.26% increase for the 3 mm nozzle compared to the 20 mm nozzle.
- Microstructural analysis revealed exceptionally strong adhesion between aggregates and binders, with polypropylene fibers aligned in a parallel pattern, contributing to the material's strength and durability.
- The study identified optimal fresh concrete properties, with a slump of 40 mm and a slump flow of 160 mm, values consistent with previous research in the field.
- Cost analysis demonstrated significant cost savings with the use of affordable materials. The cost per cubic meter of the original mix (290 EUR) was compared with various modified mixes. The highest cost was achieved with the addition of 20% silica fume, resulting in a 34.83% cost increase (476 EUR). Other cost increases include 29.31% for white cement (340 EUR), 21.38% for carbon fibers (400 EUR), 19.14% for basalt fibers (370 EUR), 22.07% for aramid fibers (396 EUR), and combinations thereof.

This research highlights the promising potential of 3D printed concrete as an economically viable alternative for construction projects. Moreover, it emphasizes the importance of optimizing concrete mixes, showcasing that cost-efficiency is not solely reliant on prefabrication but is significantly influenced by the choice of materials. These findings open up new avenues for sustainable, cost-effective, and high-performance construction practices in the future.

Author Contributions: Conceptualization, N.Ț. and D.U.; methodology, N.V. and C.O.; validation, D.U.; formal analysis, D.U.; investigation, D.U. and D.A.G.; resources, I.A.S. and Ș.V.Z.; data curation, D.U. and Ș.V.Z.; writing—original draft preparation, D.U.; writing—review and editing, N.Ț. and D.U.; supervision, I.A.S. and D.A.G.; project administration, C.O. and N.V. All authors have read and agreed to the published version of the manuscript.

Funding: This paper was realized with the support of the COMPETE 2.0 project nr.27PFE/2021, financed by the Romanian Government, Minister of Research, Innovation and Digitalization.

Data Availability Statement: The data underlying this article will be shared on reasonable request from the corresponding author.

Acknowledgments: The materials tested and characterized in this work were provided by Holcim Romania and Master Builders Solutions Romania. Holcim Romania supports and promotes research

activities related to 3D-printed constructions carried out by the Faculty of Construction and Building Services in Iasi.

Conflicts of Interest: The authors declare no conflict of interest.

References

1. Jindal, B.B.; Sharma, R. The effect of nanomaterials on properties of geopolymers derived from industrial by-products: A state-of-the-art review. *Constr. Build. Mater.* **2020**, *252*, 119028. [CrossRef]
2. Jindal, B.B.; Jangra, P. 3D Printed Concrete: A comprehensive review of raw material's properties, synthesis, performance, and potential field applications. *Constr. Build. Mater.* **2023**, *387*, 131614. [CrossRef]
3. Ungureanu, D.; Onuțu, C.; Isopescu, D.N.; Țăranu, N.; Zghibarcea, Ș.V.; Spiridon, I.A.; Polcovnicu, R.A. A Novel Approach for 3D Printing Fiber-Reinforced Mortars. *Materials* **2023**, *16*, 4609. [CrossRef] [PubMed]
4. Salah, H.A.; Mutalib, A.A.; Kaish, A.B.M.A.; Syamsir, A.; Algaifi, H.A. Development of Ultra-High-Performance Silica Fume-Based Mortar Incorporating Graphene Nanoplatelets for 3-Dimensional Concrete Printing Application. *Buildings* **2023**, *13*, 1949. [CrossRef]
5. Singh, N.; Colangelo, F.; Farina, I. Sustainable Non-Conventional Concrete 3D Printing—A Review. *Sustainability* **2023**, *15*, 10121. [CrossRef]
6. Robayo-Salazar, R.; Martínez, F.; Vargas, A.; Mejía de Gutiérrez, R. 3D Printing of Hybrid Cements Based on High Contents of Powders from Concrete, Ceramic and Brick Waste Chemically Activated with Sodium Sulphate (Na_2SO_4). *Sustainability* **2023**, *15*, 9900. [CrossRef]
7. Ma, G.; Ruhan, A.; Xie, P.; Pan, Z.; Wang, L.; Hower, J.C. 3D-printable aerogel-incorporated concrete: Anisotropy influence on physical, mechanical, and thermal insulation properties. *Constr. Build. Mater.* **2022**, *323*, 126551. [CrossRef]
8. Ma, G.; Salman, N.M.; Wang, L.; Wang, F. A novel additive mortar leveraging internal curing for enhancing interlayer bonding of cementitious composite for 3D printing. *Constr. Build. Mater.* **2020**, *244*, 118305. [CrossRef]
9. Li, Z.; Wang, L.; Ma, G.; Sanjayan, J.; Feng, D. Strength and ductility enhancement of 3D printing structure reinforced by embedding continuous micro-cables. *Constr. Build. Mater.* **2020**, *264*, 120196. [CrossRef]
10. Hudisteanu, I.; Taranu, N.; Isopescu, D.N.; Entuc, I.S.; Oprisan, G.; Ungureanu, D. Numerical analysis of intralaminar damage evolution on various composite laminates. *IOP Conf. Ser.-Mater. Sci. Eng.* **2018**, *400*, 042031. [CrossRef]
11. Hudisteanu, I.; Taranu, N.; Isopescu, D.N.; Bejan, L.; Axinte, A.; Ungureanu, D. Improving the mechanical properties of composite laminates through the suitable selection of the corresponding materials and configurations. *Rom. J. Mater.* **2017**, *47*, 252–266.
12. Shahzad, Q.; Wang, X.; Wang, W.; Wan, Y.; Li, G.; Ren, C.; Mao, Y. Coordinated adjustment and optimization of setting time, flowability, and mechanical strength for construction 3D printing material derived from solid waste. *Constr. Build. Mater.* **2020**, *259*, 119854. [CrossRef]
13. Rehman, A.U.; Lee, S.M.; Kim, J.H. Use of municipal solid waste incineration ash in 3D printable concrete. *Process Saf. Environ.* **2020**, *142*, 219–228. [CrossRef]
14. Available online: https://romfracht.com/ro/fibers/?gclid=Cj0KCQjwuLShBhC_ARIsAFod4fLouQv6ihOaNCAF9iAex2c8Y6g90XyG4GRtyNW6kr4-UBAN7HQFLjsaAgUgEALw_wcB (accessed on 5 April 2023).
15. Ibrahim, K.A.; van Zijl, G.P.A.G.; Babafemi, A.J. Influence of limestone calcined clay cement on properties of 3D printed concrete for sustainable construction. *J. Build. Eng.* **2023**, *69*, 106186. [CrossRef]
16. Alami, A.H.; Olabi, A.G.; Ayoub, M.; Aljaghoub, H.; Alasad, S.; Abdelkareem, M.A. 3D Concrete Printing: Recent Progress, Applications, Challenges, and Role in Achieving Sustainable Development Goals. *Buildings* **2023**, *13*, 924. [CrossRef]
17. 3D PotterBot 10 XL. Available online: https://3dpotter.com/printers/potterbot-10-xl (accessed on 25 October 2023).
18. *EN 12350-2:2019*; Testing Fresh Concrete—Part 2: Slump Test. European Committee for Standardization: Brussels, Belgium, 2019.
19. Tay, Y.W.D.; Qian, Y.; Tan, M.J. Printability region for 3D concrete printing using slump and slump flow test. *Compos.B Eng.* **2019**, *174*, 106968. [CrossRef]
20. *ASTM C1437-15*; Standard Test Method for Flow of Hydraulic Cement Mortar. ASTM International: West Conshohocken, PA, USA, 2015.
21. *ASTM C230/C230M*; Standard Specification for Flow Table for Use in Tests of Hydraulic Cement. ASTM International: West Conshohocken, PA, USA, 2008.
22. *SR EN 12390-3:2002*; Încercare pe Beton Întărit. Partea 3: Rezistența la Compresiune a Epruvetelor. Organismul Național de Standardizare din România: Bucharest, Romania, 2002. (In Romanian)
23. *SR EN 12390-5:2019*; Încercare pe Beton Întărit. Partea 5: REZISTENȚA la Încovoiere a Epruvetelor. Organismul Național de Standardizare din România: Bucharest, Romania, 2019. (In Romanian)
24. Bouchabou, D.; Grosset, J.; Nguyen, S.M.; Lohr, C.; Puig, X. A Smart Home Digital Twin to Support the Recognition of Activities of Daily Living. *Sensors* **2023**, *23*, 7586. [CrossRef] [PubMed]
25. Hassebo, A.; Tealab, M. Global Models of Smart Cities and Potential IoT Applications: A Review. *IoT* **2023**, *4*, 366–411. [CrossRef]
26. Hammad, M.; Jillani, R.M.; Ullah, S.; Namoun, A.; Tufail, A.; Kim, K.-H.; Shah, H. Security Framework for Network-Based Manufacturing Systems with Personalized Customization: An Industry 4.0 Approach. *Sensors* **2023**, *23*, 7555. [CrossRef]

27. Influencing Factors of Cost Calculation in C3DP. Available online: https://jwcn-eurasipjournals.springeropen.com/articles/10.1186/s13638-018-1163-9/tables/2 (accessed on 25 August 2023).
28. Ungureanu, D.; Țăranu, N.; Ghiga, D.A.; Isopescu, D.N.; Mihai, P.; Cozmanciuc, R. Diagonal Tensile Test on Masonry Panels Strengthened with Textile-Reinforced Mortar. *Materials* **2021**, *14*, 7021. [CrossRef] [PubMed]
29. Onuțu, C.; Ungureanu, D.; Isopescu, D.N.; Vornicu, N.; Spiridon, I.A. Sourcing Limestone Masonry for the Restoration of Heritage Buildings: Frumoasa Monastery Case Study. *Materials* **2022**, *15*, 7178. [CrossRef]
30. Spiridon, I.A.; Ungureanu, D.; Țăranu, N.; Onuțu, C.; Isopescu, D.N.; Șerbănoiu, A.A. Structural Assessment and Strengthening of a Historic Masonry Orthodox Church. *Buildings* **2023**, *13*, 835. [CrossRef]
31. Ungureanu, D.; Țăranu, N.; Hoha, D.; Zghibarcea, Ș.; Isopescu, D.N.; Boboc, V.; Oprișan, G.; Scutaru, M.C.; Boboc, A.; Hudișteanu, I. Accelerated testing of a recycled road structure made with reclaimed asphalt pavement material. *Constr. Build. Mater.* **2020**, *262*, 120658. [CrossRef]
32. Wu, Y.; Bian, X.; Liu, J.; Chi, R.; Chen, X. Performance Improvement and Microstructure Characterization of Cement-Stabilized Roadbase Materials Containing Phosphogypsum/Recycled Concrete Aggregate. *Materials* **2023**, *16*, 6607. [CrossRef] [PubMed]
33. Rudnicki, T.; Stałowski, P. Fast-Setting Concrete for Repairing Cement Concrete Pavement. *Materials* **2023**, *16*, 5909. [CrossRef]
34. Deng, M.; Xie, X.; Zhuo, J.; He, Y.; Wang, K. Experimental Study on the Strength and Hydration Products of Cement Mortar with Hybrid Recycled Powders Based Industrial-Construction Residue Cement Stabilization of Crushed Aggregate. *Materials* **2023**, *16*, 4233. [CrossRef]
35. Michałowska-Maziejuk, D.; Goszczyńska, B. Effectiveness of Strengthening RC Beams Using Composite Materials—An Accelerated Strengthening Method. *Materials* **2023**, *16*, 4847. [CrossRef]
36. Khan, M.I.; Abbas, Y.M. Behavioral Evaluation of Strengthened Reinforced Concrete Beams with Ultra-Ductile Fiber-Reinforced Cementitious Composite Layers. *Materials* **2023**, *16*, 4695. [CrossRef] [PubMed]
37. Shangguan, B.; Su, Q.; Casas, J.R.; Su, H.; Wang, S.; Zhao, R. Modeling and Testing of a Composite Steel–Concrete Joint for Hybrid Girder Bridges. *Materials* **2023**, *16*, 3265. [CrossRef] [PubMed]
38. Benkhaled, M.; Ouldboukhitine, S.-E.; Bakkour, A.; Amziane, S. A 1D Model for Predicting Heat and Moisture Transfer through a Hemp-Concrete Wall Using the Finite-Element Method. *Materials* **2021**, *14*, 6903. [CrossRef] [PubMed]
39. Marczyk, J.; Ziejewska, C.; Gądek, S.; Korniejenko, K.; Łach, M.; Góra, M.; Kurek, I.; Doğan-Sağlamtimur, N.; Hebda, M.; Szechyńska-Hebda, M. Hybrid Materials Based on Fly Ash, Metakaolin, and Cement for 3D Printing. *Materials* **2021**, *14*, 6874. [CrossRef] [PubMed]
40. Feng, J.; Dong, C.; Chen, C.; Wang, X.; Qian, Z. Effect of Manufactured Sand with Different Quality on Chloride Penetration Resistance of High–Strength Recycled Concrete. *Materials* **2021**, *14*, 7101. [CrossRef] [PubMed]
41. Liu, H.; Egbe, K.-J.I.; Wang, H.; Matin Nazar, A.; Jiao, P.; Zhu, R. A Numerical Study on 3D Printed Cementitious Composites Mixes Subjected to Axial Compression. *Materials* **2021**, *14*, 6882. [CrossRef] [PubMed]
42. Lauff, P.; Pugacheva, P.; Rutzen, M.; Weiß, U.; Fischer, O.; Volkmer, D.; Peter, M.A.; Grosse, C.U. Evaluation of the Behavior of Carbon Short Fiber Reinforced Concrete (CSFRC) Based on a Multi-Sensory Experimental Investigation and a Numerical Multiscale Approach. *Materials* **2021**, *14*, 7005. [CrossRef] [PubMed]

Disclaimer/Publisher's Note: The statements, opinions and data contained in all publications are solely those of the individual author(s) and contributor(s) and not of MDPI and/or the editor(s). MDPI and/or the editor(s) disclaim responsibility for any injury to people or property resulting from any ideas, methods, instructions or products referred to in the content.